



Detection of hard intermetallics in β -quenched and thermally aged Zircaloy-2 using ultrasonic measurements

T. Jayakumar, P. Palanichamy, Baldev Raj *

Metallurgy and Materials Group, Indira Gandhi Centre for Atomic Research, Kalpakkam-603 102, India

Received 8 November 1997; accepted 20 January 1998

Abstract

Zircaloy-2 is widely used for critical core components in the pressurized heavy water reactors. Components of Zircaloy-2 are usually fabricated from the β -quenched billets. Proper quenching treatment must be ensured to avoid the rejection of finished products made from Zircaloy-2. Metallographic techniques are used for this purpose. However, it is advantageous to use nondestructive testing (NDT) techniques such as ultrasonics. In this work, laboratory investigations are carried out on the feasibility for the assessment of the acceptability of the β -quenched microstructure using ultrasonic attenuation and velocity measurements in the frequency range 2–100 MHz. Precise velocity measurements with an accuracy of 0.2 ns by cross-correlation technique have been made in this study. Results indicate that low frequency (2–10 MHz) ultrasonic velocity measurements using both longitudinal and transverse waves are useful for revealing the presence of hard intermetallics. High-frequency (75 and 100 MHz) ultrasonic velocity measurements are useful for revealing the early-stage dissociation of β -quenched martensite to α -phase. Ultrasonic measurements are also correlated with hardness and density measurements in addition to microstructural features. As compared to the attenuation measurements, velocity measurements are more reliable and repeatable for microstructural characterisation of Zircaloy-2. © 1998 Elsevier Science B.V. All rights reserved.

1. Introduction

Zircaloy-2 is widely used in the pressurized heavy water reactors (PHWR). The material has a low thermal neutron capture cross-section and good strength properties at high temperatures, which make it an excellent material for nuclear reactor core components [1,2]. Among the various alloys, Zircaloy-2 and Zr–2.5% Nb alloys are widely used in the CANDU-type PHWR. The three important core components made of Zircaloy-2 are fuel cladding tubes, pressure tubes and calandria tubes [1].

One of the important steps in the fabrication route for the Zircaloy-2 components is the β -quenching of the hot extruded billets. The β -quenching treatment is given to homogenise the chemical composition and randomise the texture [3]. Many times, the β -quenching treatment is not

reproducible, leading to unacceptable microstructural conditions after β -treatment. Non-detection of such unacceptable microstructure may lead to rejection of the final products fabricated from the β -quenched billets, as they do not meet the specified properties for these products, thus leading to loss of production and wastage of manpower and money. One of the possible reasons for this unacceptable microstructural condition in the β -quenched billet is the variation in the cooling rate. Inadequate cooling rate may result in the precipitation of hard intermetallic phases, which may interfere with subsequent deformation processes applied in the fabrication route.

In Zircaloy-2, Sn, Fe, Cr and Ni are added as alloying elements for obtaining the desired mechanical properties, in addition to obtaining the required corrosion resistance in high-temperature water. The solubility of these elements (except Sn) in low temperature α -Zr phase is limited because of the unfavourable size factor and/or crystal structure considerations [3]. However, the high-tempera-

* Corresponding author. Tel.: +91-414 40 208; fax: +91-414 40 356; e-mail: tj@igcar.ernet.in

ture β -phase can dissolve these elements to appreciable extent. Among the alloying elements used in Zircaloy-2, Sn is an α -stabiliser while the Fe, Ni, and Cr are β -stabilisers. The β -quenching treatment results in α supersaturated solid solution in the form of a martensitic structure. In order to obtain only the martensite structure without any secondary phases, sufficient cooling rate should be employed. Fig. 1 gives the time–temperature transformation diagram for Zircaloy-2 [4]. From Fig. 1, an idea can be obtained on the minimum cooling rate needed during β -quenching treatment to avoid the initiation of the precipitation of hard intermetallic phases. At a temperature of about 873 K, the time required for the initiation of the precipitation of hard intermetallics is as small as a few seconds only. This clearly indicates the criticality of the cooling rate to be maintained throughout the billet volume to ensure that the hard intermetallic phases are not formed during β -quenching. It has been reported that the hard intermetallic phases do not form above 1093 K, and the time required for the onset of intermetallic precipitation can be very short, i.e., about 30 s at about 1093 K [4]. Therefore, precipitation of intermetallics is very likely if the cooling rate throughout the hot-extruded billet is not sufficient enough during quenching treatment, particularly when the billet is cooling in the temperature range where the intermetallics form. Two types (A and B) of intermetallic precipitates, as described below, have been identified in Zircaloy-2 [5]: (i) Type A precipitates: Zr–Ni–Fe intermetallic compound, spherical or ellipsoidal morphology, tetragonal structure (Zr_2Ni type) with approximate composition of $Zr_2Ni_{0.4}Fe_{0.6}$. (ii) Type B precipitates: Zr–Cr–Fe intermetallic compound, spherical or rectangular morphology with hexagonal structure ($ZrCr_2$ type). Nondestructive assessment of the acceptability of the β -quenched microstructure would help in avoidance of rejection of finished products, thus saving time and resulting in economy. At higher temperatures of aging (i.e., beyond 773 K), there is a possibility for the dissociation of martensite and the formation of small-size isolated α -phase.

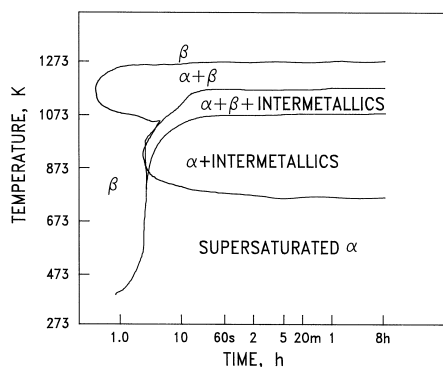


Fig. 1. Isothermal time–temperature transformation diagram for Zircaloy-2.

In this work, an attempt has been made to use ultrasonic velocity and attenuation measurements to nondestructively characterize the microstructures in Zircaloy-2, particularly the detection of the presence of hard intermetallic phases. The influence of microstructural changes due to isochronal aging for 1 h in the temperature range 473 to 973 K of β -quenched Zircaloy-2 on ultrasonic velocity and attenuation has been studied.

2. Preparation of specimens

The chemical composition (in wt%) of the Zircaloy-2 used in this study is as follows: Sn—1.62, Fe—0.18, Cr—0.1, Ni—0.06 and O—1400 ppm. Several specimens of Zircaloy-2 with the size $50 \times 25 \times 3$ mm were vacuum-sealed and given a common β -quenching treatment by heating to 1223 K and holding for 2 h, followed by water quenching. These specimens were then thermally aged for 1 h in the temperature range 473 to 973 K and air-cooled. The microstructures corresponding to these treatments simulate the microstructures obtainable by improper β -quenching treatment due to inadequacy in cooling rates. From the heat-treated specimens, three sets of specimens were prepared: one set for metallography, another for hardness, and the third for ultrasonic and density measurements. For precise ultrasonic velocity measurements, surfaces of the specimens have been made plane-parallel to within $\pm 3 \mu\text{m}$.

3. Experimental

3.1. Metallography

Metallography on these specimens was carried out to reveal the microstructures. The etchant used consists of 7% hydrogen fluoride, 42% nitric acid and 51% water.

3.2. Hardness measurements

Hardness of the specimens was obtained by Vicker's hardness tester using a 10-kg load. At least five measurements were made for each specimen.

3.3. Density measurements

The density of the specimens was measured using Archimedes principle. All the weight measurements were made using the model Liber AEG-220 balance from M/s Shimadzu, Japan. The accuracy for the weight measurements is ± 0.0001 g. The liquid used for suspending the specimens is di-*n*-butyl phthalate having a density of 1.042 g/cc. For each specimen, a set of three readings was taken.

3.4. Ultrasonic velocity measurements

The block diagram of the experimental arrangement for attenuation and velocity measurements is shown in Fig. 2. A pulser–receiver model 10150PR supplied by M/s Accu-Tron, USA, a 500-MHz Tektronix oscilloscope model 524A and a PC/AT 486 were used for r.f. signal recording. Precise transit time measurements (with an accuracy of ± 0.2 ns) were carried out by cross-correlation technique [6,7] using longitudinal waves in the frequency range 2 to 100 MHz and transverse waves with 4 MHz frequency. Various steps involved in the ultrasonic transit time measurements are: (i) acquisition, digitisation and storage of the r.f. signal from the transducer, (ii) application of the window technique to select any two desired back wall echoes, (iii) cross-correlation of the two echoes for finding the approximate time delay, (iv) adopting cubic spline interpolation method to the peak portion of the cross-correlated function to arrive at the exact time delay, and (v) calculating the ultrasonic velocity from the specimen thickness and the measured time delay. Reference 7 gives the complete details of the cross-correlation technique employed.

3.5. Determination of elastic moduli

The following relations between elastic moduli, ultrasonic velocities, density and Poisson's ratio have been employed:

$$E = \rho V_l^2 \left[\frac{(1 - 2\nu)(1 + \nu)}{(1 - \nu)} \right],$$

$$G = \rho V_t^2,$$

where E is the Young's modulus; G is the shear modulus; ρ is the mass density of the material; V_l is the longitudinal wave velocity; V_t is the shear wave velocity; ν is the Poisson's ratio (of the order of 0.38 assumed for Zircaloy-2).

3.6. Ultrasonic attenuation measurements

Low-frequency attenuation measurements were carried out using 2 MHz contact and 10 MHz immersion type transducers and high-frequency attenuation measurements were carried out using 25, 50, 75 and 100 MHz contact

delay line transducers. Care was taken to avoid the problem of near field effects. A constant pressure was maintained between transducer and specimens during the contact measurements. Among the various available couplants, filtered machine oil was found to be more suitable to get steady back wall echo train in the oscilloscope screen. Peak amplitudes of first and second back wall echoes from specimens were used for the calculation of the attenuation coefficients. In the case of measurements with immersion transducer, these echoes were identified as signals that appear after the reflection signal from specimen top surfaces. In case of delay line contact transducers, these echoes were identified as signals which appear after the delay line echo signals.

4. Results and discussion

Fig. 3a shows the photomicrograph of the β -quenched microstructure of the Zircaloy-2 specimen. Fig. 3b,c show the microstructures of the specimens aged at 773 and 973 K, respectively. It was reported that martensite structure is retained up to about 773 K in various zirconium alloys and contributes to the strength [8]. It is found in the present study that all the heat-treated specimens retained essentially the martensite structure. In the specimens aged at 773 K (Fig. 3b), fine precipitates could be seen. These precipitates are the hard intermetallics discussed earlier. Similar precipitation is seen in the case of specimens aged at 673 and 873 K also. The specimen aged at 973 K shows the indication for the formation of α -phase (as marked in the photomicrograph 3c) in the martensite structure. Fig. 4 shows the variation in hardness with the aging temperature. The hardness is found to increase with aging temperature and then decreases at higher aging temperature with a broad maximum in the temperature range 673 to 873 K. This temperature range corresponding to the broad maximum in the hardness is the same where intermetallic precipitates are observed by optical metallography, thus confirming that the precipitation of hard intermetallics, as seen in the microstructures, led to the increase in the hardness of the material. The broad maximum in the hardness indicates that (at three temperatures i.e., 673, 773 and 873 K), most of the precipitation took place within 1 h of aging used. The variation in density with aging temperature is almost similar to that of hardness variation.

Fig. 5 shows the variation in ultrasonic velocities using normal beam 2 MHz longitudinal wave and 4 MHz transverse wave transducers. It can be seen from Fig. 5 that there is a decrease in the velocity with aging temperature up to 773 K and further increase in the aging temperature resulted in the increase in the ultrasonic velocity. This typical trend in the ultrasonic velocity measurements was obtained even for the longitudinal waves with different frequencies up to 50 MHz. It can be noted that the

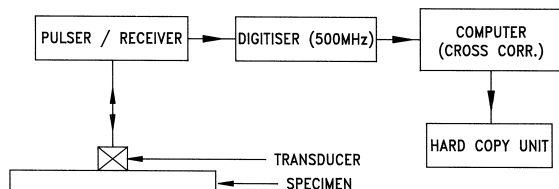
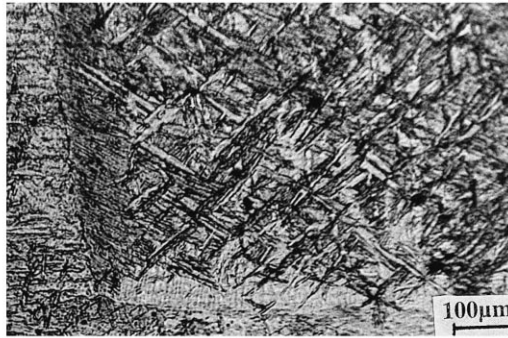


Fig. 2. Block diagram of the experimental set-up.

(a) β -quenched showing martensitic structure.



(b) β -quenched and aged at 773K showing hard intermetallics.



(c) β -quenched and aged at 973K showing precipitates of alpha Zirconium.

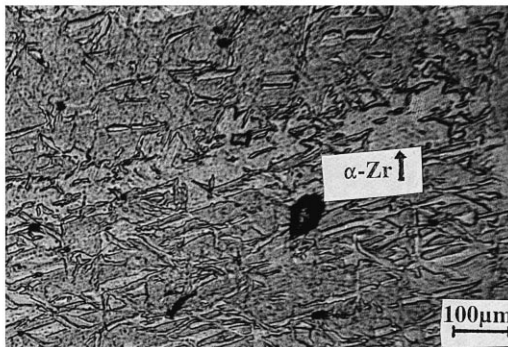


Fig. 3. Photomicrographs of β -quenched and thermally aged Zircaloy-2. (a) β -quenched, (b) β -quenched and aged at 773 K, and (c) β -quenched and aged at 973 K.

maximum reduction in the velocity due to the presence of hard intermetallics in β -quenched and aged Zircaloy-2 is 1.2% in case of transverse waves, whereas it is 0.7% in case of longitudinal waves. Hardness measurements (Fig. 4) indicated an opposite trend to the velocity measurements, i.e., an increasing trend up to the aging temperature of 773 K, and beyond this temperature, a sharp decrease in the hardness was observed. Density measurements indicated almost a similar behavior to that of hardness measurements up to 773 K. Beyond 773 K, saturation in the density was observed.

In the β -quenched condition, all the solute elements like Sn, Fe, Ni, Cr etc. would be in the solid solution. During the aging process, as the temperature of the aging

is increased, the solute elements will come out of the solid solution and precipitate as hard intermetallic phases. However, aging at still higher temperatures, the increased solubility of the solute elements in the zirconium matrix would result in the reduction in the amount of precipitates formed or may not form depending on the temperature of aging and the solute content. Therefore, the extent of formation of intermetallic phases would be maximum at an intermediate aging temperature. This explains the observed minimum in the velocity and the maximum in the hardness and density with the temperature of aging in Zircaloy-2. Earlier studies made by Bush et al. [9] indicated that secondary hardening takes place during recrystallisation of cold-worked Zircaloy-2 at 723 K. It was also observed that

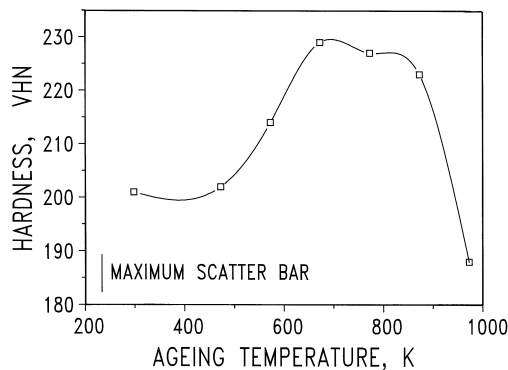


Fig. 4. Variation of hardness with aging temperature in β -quenched Zircaloy-2.

straining at room temperature and at 533 K had no effect on the slope of the log critical strain (for recrystallisation) vs. temperature plot, whereas straining at 755 K did change the slope [10]. The reason for these types of behaviour in the temperature range 723–755 K is attributed to the precipitation of hard intermetallic phases. These studies also support the metallographic observations of formation of precipitates in the specimens aged at 773 K (Fig. 3b) and also the interpretations made to explain the variation in the velocity, hardness and density with the temperature of aging.

Fig. 6 shows the variation in the Young's modulus and the shear modulus with the temperature of aging. It can be seen from Fig. 6 that there is a distinct minimum in both the moduli at 773 K. The overall modulus of the material with multiple phases is decided by the volume fraction and modulus of individual phases [11]. Partial removal of the elements like Fe, Ni and Cr from the matrix for forming the hard intermetallics would alter its modulus. Since the volume fraction of the hard intermetallics is very small, its influence on the overall modulus of the material is expected to be negligible. Hence, only the change in the modulus of the matrix due to its altered composition

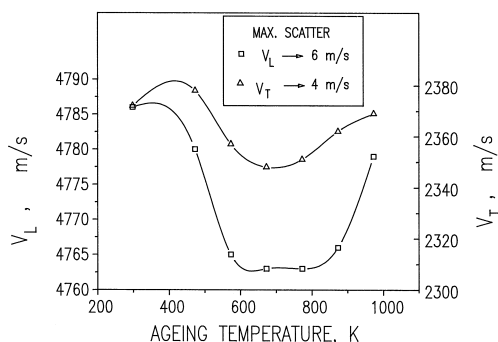


Fig. 5. Variation in longitudinal 2 MHz (V_L) and shear wave 4 MHz (V_T) velocities with aging temperature in β -quenched Zircaloy-2.

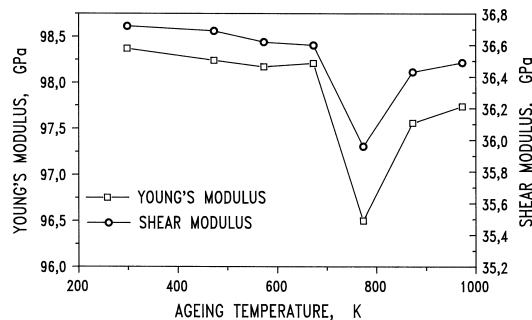


Fig. 6. Variation in Young's and shear moduli with aging temperature.

(consequent to removal of Fe, Ni and Cr) would determine the overall modulus of the material. It can be inferred from our results that the change in the composition of the matrix reduces the overall modulus.

Longitudinal ultrasonic velocity measurements were also made at 50, 75, and 100 MHz frequencies. Fig. 7 shows the variation in the longitudinal velocity as a function of aging temperature at frequencies from 25 to 100 MHz. Up to 50 MHz, the trend in the velocity variation with aging temperature is similar to that at lower frequencies. However, for 75 and 100 MHz frequencies, measurements showed a continuous decrease in the velocity with aging temperature. This continuous decrease in the velocity at 75 and 100 MHz frequencies (results shown only for 100 MHz in Fig. 7) in the specimens aged at higher temperatures (beyond 773 K) has been attributed to initiation of dissociation of β -quenched martensite and formation of small size and isolated α -phase ($\approx 100 \mu\text{m}$ in size) at higher temperatures (Fig. 3c). At lower frequencies, the absence of continuous decrease in the velocity beyond 873 K is attributed to long wavelength of the ultrasonic waves,

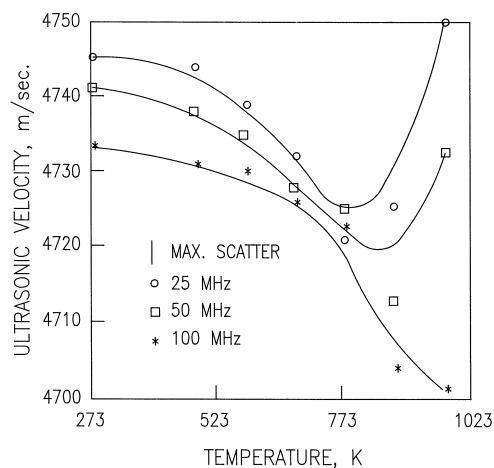


Fig. 7. Variation in longitudinal velocity (V_L) with aging temperature for 25, 50 and 100 MHz ultrasonic frequencies.

and hence lack of appreciable interaction between the ultrasonic waves and the small size, and very low volume fraction of the isolated α -phase. In a separate study [12], the velocity measurements made in α -phase of the same material, indicated a value of 4770 m/s for longitudinal waves at 2 MHz. This is lower than the velocity of the β -quenched Zircaloy-2 by about 15 m/s (i.e., 4785 m/s). This explains the reduction in the velocities at higher frequencies (75 and 100 MHz) in specimens aged at higher temperatures and containing isolated and small size α -phase in the specimen aged at 973 K. From Fig. 3c, it is seen that α -phase constitutes over 12–15% of the total volume. Presence of α -phase led to decrease in the ultrasonic velocity by about 8–10 m/s as compared to that for the β -quenched condition due to the presence of α -phase. In terms of percentage variation in ultrasonic velocity, it is 0.17–0.21%. This study points out that detection and

presence of α -phase is possible by employing ultrasonic velocity measurements.

Fig. 8a shows the variation in the ultrasonic attenuation with aging temperature for low frequencies (2 and 10 MHz) and Fig. 8b shows the attenuation of longitudinal waves as a function of aging temperature at higher frequencies (25, 50 and 100 MHz). The change in the attenuation due to aging is marginal at 2 MHz. At all other frequencies, variation in the attenuation with aging temperature generally shows an opposite trend to that of the velocity, i.e., an increasing trend in the attenuation with aging temperature and reaches a peak at 873 K and beyond that, attenuation decreases at further aging temperature (973 K). The scatter-band for low-frequency attenuation measurements is high, i.e., 0.04 dB/mm even in the case of immersion-type measurements, and hence low-frequency attenuation measurements cannot be employed reliably for characterisation of different microstructures in the quenched and aged specimens. However, the scatter band in attenuation measurements at higher frequencies (25, 50 and 100 MHz) is relatively less, i.e., 0.005 dB/mm, and the observed trend can be taken into account in interpreting the results with respect to the changes in the microstructure. The increasing trend in the attenuation up to 873 K is attributed to precipitation of hard intermetallics. Subsequent reduction in the attenuation at 973 K is attributed to reduced amount of precipitation of intermetallics at higher temperatures. The reduction in the attenuation occurs in spite of precipitation of a small amount of α -Zr. Although, it is possible to use attenuation measurements, for characterisation of the microstructural features in the β -quenched and aged Zircaloy-2, the overall change in the attenuation is small and it would be difficult to employ attenuation measurements even at high frequencies, unless large number of measurements are made to avoid statistical variation in the measurements. On the other hand, ultrasonic velocity measurements are more reliable.

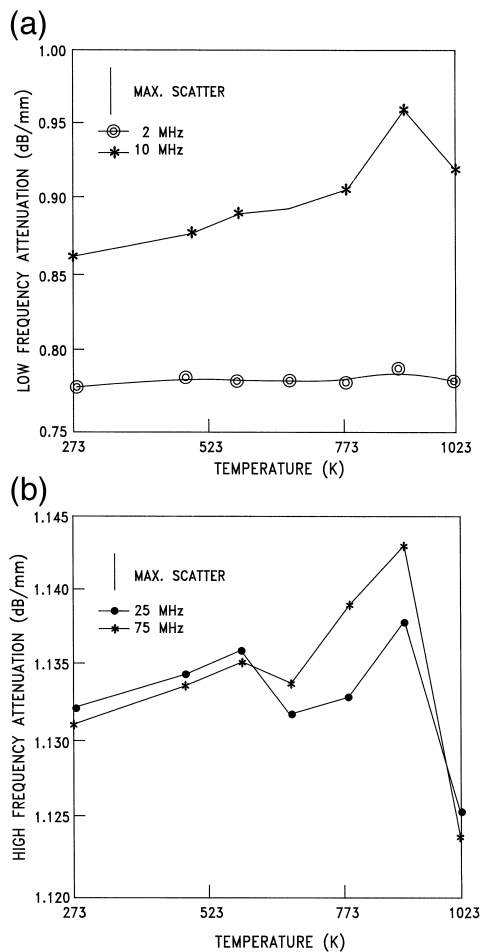


Fig. 8. (a) Ultrasonic attenuation as a function of aging at ultrasonic frequencies 2 and 10 MHz. (b) Ultrasonic attenuation as a function of aging temperature at ultrasonic frequencies 25 and 75 MHz.

5. Conclusion

Ultrasonic velocity measurements are useful for detection of the presence of hard intermetallic phases in beat-quenched Zircaloy-2, as this condition would lead to a reduction in the velocity in the frequency limit up to 50 MHz. By specifying a minimum velocity as a quality control parameter for the beat-quenched Zircaloy-2, material with unacceptable microstructural conditions can be identified for recommending to repeat the beat-quenching treatment. While the low-frequency velocity measurements reveal the presence of hard intermetallics, high-frequency (75 and 100 MHz) velocity measurements would also reveal early stage dissociation of β -quenched martensite to α -phase. On the other hand, ultrasonic attenuation mea-

surements do not reveal such definite results. Attenuation measurements made above 10 MHz frequency could also reveal the presence of hard intermetallics.

Acknowledgements

We express our sincere thanks to Mr M. Narayana Rao, Nuclear Fuel Complex, Hyderabad for providing the Zircaloy-2 material. We also wish to thank Mr P. Kalyanasundaram, Head, DPEND for many useful discussions. We are grateful to Dr Placid Rodriguez, Director, IGCAR for constant encouragement and support.

References

- [1] R. Krishnan, M.K. Asundi, Proc. Indian Acad. Sci. (Eng. Sci.) 4 (1981) 41.
- [2] D.G. Douglas, The Metallurgy of Zirconium, Atomic Energy Review Supplement, 1971.
- [3] M.K. Asundi, S. Banerjee, Proc. Symp. Nuclear Fuel Fabrication (NUFAB-88), Board of Research in Nuclear Sciences, Bhabha Atomic Research Centre, Bombay, December 1988, p. 201.
- [4] G. Oestberg, *Jornknot Ann.* 145 (1961) 119.
- [5] P. Chemdle, D.B. Knorr, J.B. Van der Sande, R.M. Pelloux, *J. Nucl. Mater.* 113 (1983) 58.
- [6] D.R. Hull, H.E. Kautz, A. Vary, *Mater. Eval.* 43 (1985) 1455.
- [7] B.P.C. Rao, T. Jayakumar, D.K. Bhattacharya, B. Raj, *J. Pure Appl. Ultrasonics* 15 (1993) 53.
- [8] S. Banerjee, S. Vijayakar, R. Krishnan, *J. Nucl. Mater.* 62 (1976) 229.
- [9] S.H. Bush, R.S. Kemper, Recovery and recrystallisation of Zirconium and its alloys—Part 3, Annealing effects in Zircaloy-2 and Zircaloy-3, HW-69680, 1961.
- [10] J.C. Boakes, *Trans. AIME* 218 (1960) 1603.
- [11] Z. Ondracek, *Werkstofftech* 9 (1978) 31.
- [12] T. Jayakumar, PhD thesis, Univ. of Saarland, Saarbruecken, 1996.